Journal of Geophysical Research: Oceans

RESEARCH ARTICLE
10.1029/2018JC014218

The Impact of Agulhas Leakage on the Central Water Masses in the Benguela Upwelling System From A High-Resolution Ocean Simulation

Nele Tim[1,2], **Eduardo Zorita**[2], **Franziska U. Schwarzkopf**[3], **Siren Rühs**[3], **Kay-Christian Emeis**[1,2], **and Arne Biastoch**[3]

[1]Institute for Geology, University of Hamburg, Hamburg, Germany, [2]Institute of Coastal Research, Helmholtz-Zentrum Geesthacht, Geesthacht, Germany, [3]GEOMAR Helmholtz Centre for Ocean Research Kiel, Kiel, Germany

Key Points:
- Agulhas Current water largely contributes to central water masses in the Benguela upwelling region
- The central water mass in North Benguela is twice as old as the central water mass in South Benguela
- Ventilation of Benguelan central water masses takes place mainly southwest of Cape of Good Hope

Correspondence to:
N. Tim,
nele.tim@hzg.de

Citation:
Tim, N., Zorita, E., Schwarzkopf, F. U., Rühs, S., Emeis, K.-C., & Biastoch, A. (2018). The impact of Agulhas leakage on the central water masses in the Benguela upwelling system from a high-resolution ocean simulation. *Journal of Geophysical Research: Oceans*, *123*. https://doi.org/10.1029/2018JC014218

Received 28 MAY 2018
Accepted 6 DEC 2018
Accepted article online 9 DEC 2018

Abstract We analyze the contribution of the Agulhas Current on the central water masses of the Benguela upwelling system (BUS) over the last decades in a high-resolution ocean simulation driven by atmospheric reanalysis. The BUS is an Eastern Boundary Upwelling System where upwelling of cold nutrient-rich water favors biomass growth. The two distinct subregions, North and South Benguela, differ in nutrient and oxygen properties of the upwelling water mass. Our analysis indicates that the contribution of Agulhas water to the upwelling is very strong in both subregions. Although the water masses feeding the upwelling have a common origin, their pathways are distinct in both regions. Whereas for the central waters of South Benguela the path is rather direct from where it is formed, the central waters of North Benguela takes a longer route through the equatorial current system. Not only the travel time from the Agulhas Current to the BUS is longer but also the central water mass is twice as old for the northern part when compared to the southern. Our analysis traces the pathways, history, and origin of the central water masses feeding upwelling in the BUS and emphasizes the direct impact of the Agulhas Current on the upwelling region. The variability of that link between the Indian Ocean and the South Atlantic is likely to change the nutrient and oxygen content, as well as temperature and salinity of the water masses in the upwelling region.

Plain Language Summary This study investigates the link between two important ocean circulation systems in the South Atlantic-Indian Ocean sector: the Benguela upwelling system (BUS) and the Agulhas Current. In the BUS, located off southwest Africa, cold nutrient-rich water is transported to the surface from deeper layers, leading to high productivity. The BUS has two distinct parts, North Benguela water masses is nutrient rich, and oxygen poor, South Benguela water mass has higher oxygen concentrations. The Agulhas Current, flowing along the southeast coast of Africa, leaks into the South Atlantic Ocean south of the BUS. We assess the contribution of Agulhas water to the water masses in North and South Benguela, the travel time and pathways of the water masses into the upwelling regions. For this purpose, we analyze a global high-resolution ocean simulation. Our analysis reveals that the contribution of Agulhas water is high, in both parts of the BUS. The South Benguela water reach the upwelling region on a short route from the Cape Basin and the Brazil-Malvinas Confluence Zone. The North Benguela water, in contrast, takes a longer way by traveling through the whole South Atlantic. This leads to lower oxygen concentrations in North Benguela.

1. Introduction

The Agulhas Current is the western boundary current of the South Indian Ocean (Beal & Bryden, 1997). It transports warm and saline water originating from the Mozambique Channel and East Madagascar Current southwestward along the coast of Mozambique and South Africa. When reaching the southern tip of the African continent, most of the water turns eastward back into the Indian Ocean with the Agulhas Return Current (Beal et al., 2011). A small fraction, however, leaves the Agulhas System and flows westward into the Atlantic Ocean (Gordon, 1986). This so-called Agulhas leakage is not only a source of warm and saline water for the South Atlantic and therefore an important part of the global thermohaline circulation (Gordon, 1986; Gordon et al., 1992), it may also feed with its nutrient rich water masses the Benguela upwelling system

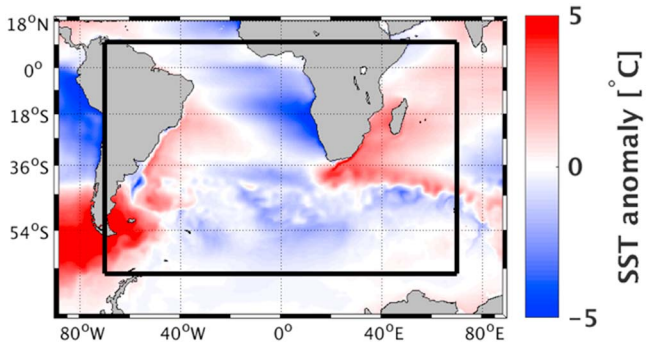

Figure 1. Model domain of the nest with 1/20° resolution (black box) of the global simulation INALT20 with 1/4° resolution outside the nest domain. Color shading indicates sea surface temperature (SST) anomaly in degrees Celsius of the global base model with regard to the zonal mean of the South Atlantic and Indian Ocean, averaged over the whole simulation period (1958–2009).

(BUS; Gordon et al., 1992). The BUS is one of the four important Eastern Boundary Upwelling Systems (EBUSs) that support a large fraction of the global ocean primary production (Shannon, 1985). Here we assess the influence of the Agulhas leakage on the BUS in a high-resolution ocean simulation and investigate by which pathways the central water masses of North and South Benguela enter the upwelling system.

Eastern South Atlantic Central Water (ESACW) is formed when Agulhas leakage water mixes in the Cape region with the South Atlantic Central Water (SACW; Mohrholz et al., 2008). The SACW itself is formed in the Brazil-Malvinas Confluence Zone in the western South Atlantic off Argentina and Uruguay (Stramma & England, 1999). Here water is subducted in the confluence of the southward Brazil Current and the northward Falkland Current. The SACW is then transported eastward with the South Atlantic Current toward the African continent and equatorward with the Benguela Current. In this study we adopt the definition according to their T-S characteristics in the Angola Dome and the Cape Basin, respectively, as done by Poole and Tomczak (1999) and Mohrholz et al. (2008). According to this point of view SACW is defined by the T-S range of 8.00–16.00 °C, 34.72–35.64 psu and ESACW by the T-S range of 5.95–14.41 °C, 34.41–35.30 psu.

The two water masses SACW and ESACW are the central water masses tapped by the BUS. The BUS is located at the coasts of Angola, Namibia, and South Africa. As all other EBUSs (California, Humboldt, and Canary upwelling systems) it is driven by the trade winds. The equatorward, coastal-parallel winds in the subtropics induce offshore transports of surface water along the coast. Upwelling water balances the offshore flow with cold and nutrient-rich waters from deeper layers (Bakun et al., 2010). The Benguela upwelling region is bounded by the Angola-Benguela-Front at around 15–17°S in the north and the Cape region at 34°S in the south. The Lüderitz upwelling cell at 27°S separates the upwelling system into a northern and a southern part (Tim et al., 2015) with distinct characteristics and seasonality. Observational studies suggest that the central waters of the South Benguela region are dominated by ESACW, whereas central waters in North Benguela are mainly fed by SACW (Mohrholz et al., 2008). Its high productivity and rich marine resources make the Benguela upwelling area a region of high ecological and economic interests (Pauly & Christensen, 1995). Records of changes in the upwelling ecosystems and productivity on interannual and interdecadal time scales thus prompt our investigation of the linkage between the upwelling system and the Agulhas leakage.

Previous studies suggest that position and intensity of the westerlies over the Indian Ocean impact the Agulhas leakage (Biastoch & Böning, 2013; Biastoch et al., 2009; Durgadoo et al., 2013). The midlatitude westerlies are the prevailing winds over the Agulhas leakage region. The intensification of the westerlies in the recent past causes an increase in Agulhas leakage (Biastoch et al., 2009; Durgadoo et al., 2013). These variations in the Agulhas leakage are candidate processes to change the composition of central water masses in the Benguela upwelling region. They possibly determine if upwelling water is oxygen rich and young with a significant amount of preformed nutrients to make the upwelling system a sink for atmospheric CO_2, or oxygen poor with dominant recycled nutrients and high CO_2 supersaturation that makes the upwelling system a source for atmospheric CO_2. The oxygen, nutrient, and CO_2 content are essential for the productivity and ecosystem of the upwelling region and for the climate system.

Our working hypothesis, based on Poole and Tomczak (1999) and Mohrholz et al. (2008), is that the water mass in North Benguela is mainly SACW that is older than the feed water in the southern Benguela due to the longer pathway from its formation in the confluence region to the northern upwelling region. The water mass is transported northwestward with the Benguela Current toward the equator and then eastward with the Equatorial Undercurrent and/or Counter Current. Its long way through the South Atlantic is associated with collection of nutrients and CO_2 and loss of oxygen by respiration and mineralization of sinking organic matter. The major central water mass in South Benguela, in contrast, is the ESACW, which would be younger due to the shorter travel path from the formation region in the southwest Atlantic. The zonal anomaly of sea surface temperature (Figure 1) exhibits the Benguela upwelling region off the southwest coast of Africa with its low temperatures as well as the two hypothesized source regions, the Brazil-Malvinas Confluence Zone in the southwestern Atlantic and the Agulhas Current system, both marked by warm temperature anomalies.

The two studies of Poole and Tomczak (1999) and Mohrholz et al. (2008) are based on observational data sets with low temporal and spatial resolution. A validation of this hypothesis in a multidecadal high-resolution ocean simulation has, to our knowledge, not been performed yet and is subject of this study.

Our approach is based on Lagrangian analysis of the trajectories of water parcels advected with ocean currents (see section 2) simulated with an eddy-rich ocean model forced by atmospheric reanalysis for the period 1958–2009. It aims to quantify the contribution of the Agulhas Current on the central water masses of the BUS and to clarify the pathways and the ages of these water masses. A high-resolution model simulation is necessary to reliably represent the mesoscale variability of the Agulhas Current and the Agulhas leakage (Biastoch et al., 2008).

Previous studies based on model simulations analyze the impact of the Agulhas leakage on the western boundary systems of the tropical Atlantic Ocean (Castellanos et al., 2017) and on the North Atlantic (Rühs et al., 2013), its correlation with the Atlantic multidecadal Oscillation (Biastoch et al., 2015), its contribution to tropical Atlantic warming (Lübbecke et al., 2015), the source water of the leakage (Durgadoo et al., 2017), and the contribution of Agulhas water to the Benguela Current (Veitch & Penven, 2017). We focus on the amount of Benguela central water masses originating from the Agulhas Current and the Brazil-Malvinas Confluence Zone, the pathways of the water masses into the upwelling region, and their age. While the physical ocean model used here does not include a biogeochemical submodel, origin and age (travel time after last ventilation) of central water masses are used as an indication on nutrient and oxygen content of the water masses in the Benguela upwelling region.

2. Data and Methods

2.1. Model Simulation

For our analysis we use a hindcast experiment with the global nested ocean-only configuration INALT20 of the NEMO model (Madec, 2008), a successor of INALT01 (Durgadoo et al., 2013). INALT20 consists of a global base model (ORCA025; Barnier et al., 2006) with a tripolar Arakawa-C grid and at an eddy-permitting horizontal resolution of 1/4° and a therein embedded nest (AGRIF; Debreu et al., 2008) covering the area 70°W to 70°E and 10°N to 63°S with a resolution of 1/20°. This eddy-resolving nest provides the advantage, among others, to realistically simulate the greater Agulhas system, including the region where the Agulhas rings are formed in the retroflection area, entering the Atlantic Ocean as Agulhas leakage. The nesting is two-way, allowing the nest not only to receive information from the global base model at its boundaries but also to transport the effect of mesoscale processes outside the nest domain. Simulated fields were stored as 5-daily means, covering the period 1958 to 2009. This hindcast simulation was driven by the atmospheric COREv2-forcing (Large & Yeager, 2009), and it was preceded by an interannually forced 30 years spin-up.

2.2. Observational Data

We compare the model output with the ocean temperature and salinity of the World Ocean Atlas 2013 version 2 (WOA13) data set (Boyer et al., 2013). WOA13 is an observation-based, gridded data set interpolated to standard depth levels provided by the National Centers for Environmental Information (NCEI) of NOAA (National Oceanic and Atmospheric Administration). The decadal average from 1995 to 2004 of temperature and salinity are analyzed with regard to the central water masses and possible model biases. WOA13 has a horizontal resolution of 1/4° on 102 vertical levels.

2.3. Lagrangian Analysis of the Model Output

Here we analyze the three-dimensional, time-evolving, and volume-conserving velocity fields from the nested region of the INALT20 hindcast (described in section 2.1) by means of off-line Lagrangian analyses performed with the ARIANE tool, as described in Blanke and Raynaud (1997) and Durgadoo et al. (2017). Lagrangian analyses have been widely used to analyze the simulated oceanic flow field of general circulation models (van Sebille et al., 2018). Large sets of Lagrangian trajectories were calculated by advecting virtual fluid parcels (small volumes of maximal 0.01 Sverdrup [Sv]) along analytically computed streamlines, representing volume transport pathways. This provides the advantage of obtaining identical trajectories when calculating forward and backward in time.

Two types of analysis are available within this tool, the *quantitative* and *qualitative* modes: In quantitative mode, an initial geographical section is defined and a number of water parcels, proportional to the velocity across this section, is seeded at every time step and their trajectories are calculated forward or backward in time using the simulated current transports. As the parcels reach one of the predetermined sampling sections,

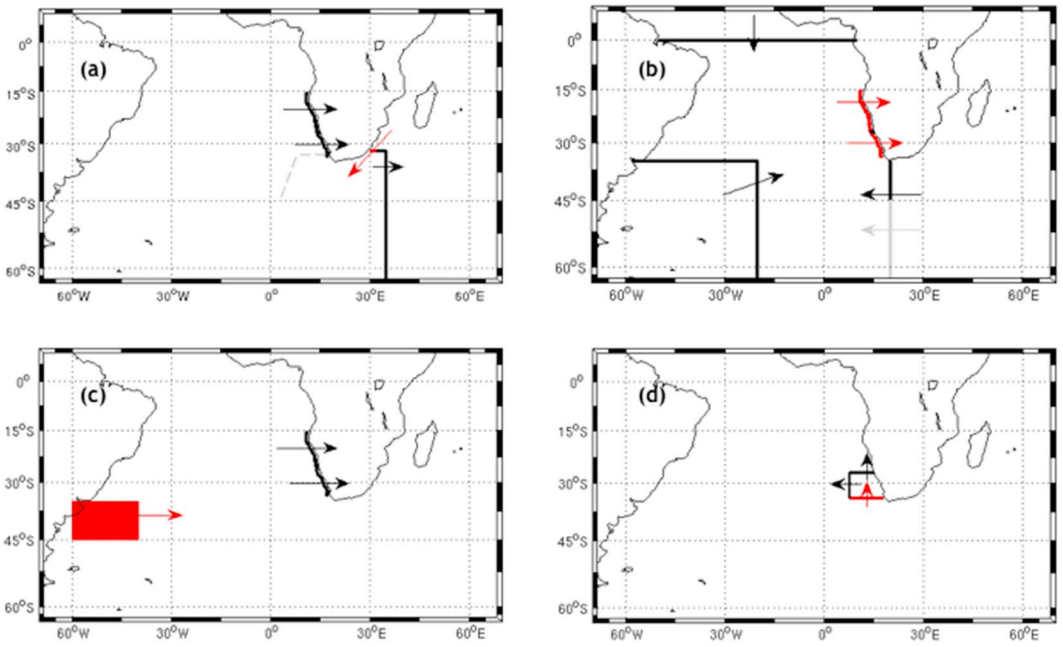

Figure 2. Schematic map of initial (seeding) sections in red and final (sampling) sections in black of the Agulhas-Benguela experiment (a), where the dashed gray line indicates the Good Hope Line (representing the leakage), the North and South Benguela experiments (b), the Formation experiment (c), and the Lüderitz experiment (d). Arrows indicate the direction of transport at seeding and sampling sections.

their associated transports are summed up yielding the total transport from the release to the different sampling sections. This is a common strategy used to quantify Lagrangian connectivity (e.g., Biastoch et al., 2008, 2009; Durgadoo et al., 2017; Rühs et al., 2013). Parcels reaching a sampling section are not further tracked. Thus, in this quantitative mode, the results provide the volume of water and amount of parcels that reach the first predefined sampling section, without considering that the parcels might arrive at another sampling section later on.

In qualitative mode, the whole trajectory of each parcel is stored, along with the ambient temperature and salinity at each position. Again, parcels can be tracked forward or backward in time. In contrast to the quantitative mode, in which the calculation of the trajectories is stopped when a parcel reaches a sampling section, in the qualitative analysis the trajectories are calculated for the whole period of the Lagrangian experiment. If the model simulation period is deemed not long enough for the analysis of low frequency variability or long paths the parcels can continue to travel through the ocean using the simulated velocities for several cycles of the Lagrangian analysis. When cycling is needed to capture the time parcels need traveling through the South Atlantic, parcels are cycled using the ad hoc method as described by, among others, van Sebille et al. (2018). For pathways calculated forward, if the end of the simulation period 2009 is reached, parcels are further tracked by starting again with the velocity fields of year 1958. For pathways calculated backward this is done reversely, so that parcels reaching the 1958 are further tracked by using velocities of the year 2009 and before in reverse order. Parcels are seeded every model output time step (every 5 days) throughout the seeding year. As the simulation domain is limited to the model nest, parcels disappear when reaching the border of the nest region.

For the analyses presented in this paper, we chose the following setups:

- Agulhas-Benguela: experiment to study the amount of Agulhas water entering the BUS. Seeding in the Agulhas Current at 32°S and between the eastern coast of South Africa and 32°E in all model layers, in the years 1969, 1979, 1989, 1999, and 2009, calculating forward for 70 years in quantitative mode (Figure 2a). As seeding is proportional to the strength of the current and the southward current is dominating this section, the parcels will not be spread homogeneously throughout the water column. Choosing different starting dates for seeding has the purpose to cover interannual variations and generating robust results. Sampling sections are here the two upwelling regions as defined in the next paragraphs, a section eastward of the seeding

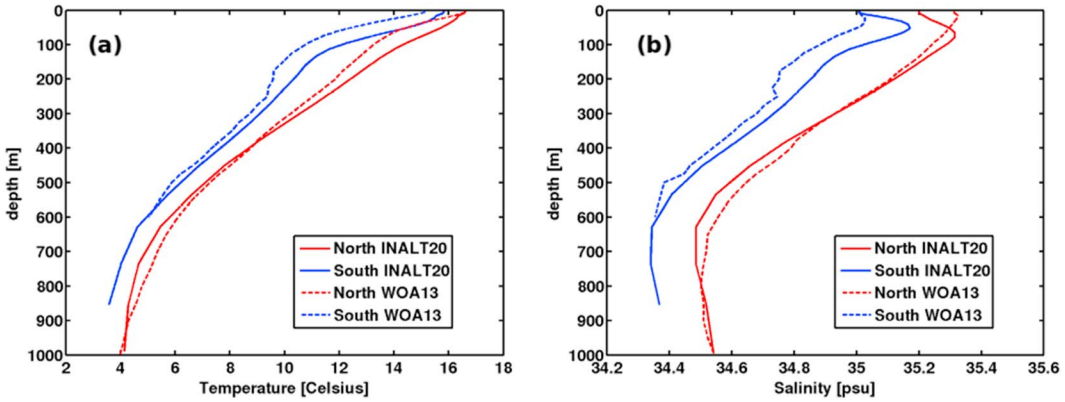

Figure 3. Profile of mean temperature (a) and salinity (b) of INALT20 (solid) and WOA13 (dashed) for North Benguela (red curves, 15°S to 27°S) and South Benguela (blue curves, 27°S to 34°S) between 100 km offshore and the coast, over the decade 1995–2004, interpolated to 1-m-depth intervals.

section at 32°S until 35°E, and a north-south transect at 35°E from 32°S until the southern end of the nest domain at 63°S.

- North Benguela: experiment to analyze the origin and pathways of the central water mass in North Benguela. Parcels are seeded between 15°S and 27°S, 100 km offshore in the temperature and salinity range of the SACW (8.00–16.00 °C, 34.72–35.64 psu; Mohrholz et al., 2008), in the same years as in the Agulhas experiments and calculating backward for 70 years in quantitative mode. Sampling sections are the southernmost tip of the African continent representing the leakage (20°E between the coast and 45°S), the equator and a section embracing the Brazil-Malvinas Confluence Zone, the formation region, as described in the corresponding experiment (60° to 20°W, 63° to 35°S; Figure 2b). For the qualitative mode we use the starting positions of the experiment in quantitative mode seeding in the last year (2009), calculating backward over the whole period.
- South Benguela: experiment to analyze the origin and pathways of central water mass in South Benguela. Seeding between 27°S and 34°S, 100 km offshore in the temperature and salinity range of the ESACW (5.95–14.41 °C, 34.41–35.30 psu; Poole & Tomczak, 1999), in the same years as in the other experiments, calculating backward for 70 years in quantitative mode. Sampling sections as well as the setup of the qualitative mode experiment are the same as for North Benguela (Figure 2b).
- Mixed-Layer run: experiment to locate the last mixed-layer contact of central water masses. Seeding in North and South Benguela (as described above) in quantitative mode with one backward cycle over the simulation period and having only the mixed-layer depth as sampling criterion where the parcels end.
- Formation region: experiment to study pathway of water from the Brazil-Malvinas Confluence Zone. Seeding between 35°S and 45°S and 40°W and 60°W within depths between 100 and 500 m, in the first year (1958), and calculating forward over the whole period in qualitative mode (Figure 2c). The region used as formation region has been chosen from previous studies (Stramma & England, 1999) and from the analysis of temperature and salinity latitude-depth variations of INALT20 and WOA13 (not shown). This analysis identifies the latitudinal position of the subduction region, which is largely covered by the chosen latitudinal range from 35°S to 45°S. Furthermore, the results of the backtracking of South Benguela parcels supports the location of the formation region within the selected area.
- Lüderitz: experiment to quantify water crossing the Lüderitz upwelling cell that separates North and South Benguela. Seeding at 34°S between the western coast of South Africa and 8°E in all depths in the first year (1958, and calculating forward over the whole simulation period in quantitative mode). Sampling sections are here the Lüderitz cell at 27°S between the coast and 8°E and a north-south orientated line in the west (at 8°E) between 27°S and 34°S (Figure 2d).

Seeding and sampling sections of the experiments in quantitative mode are shown in Figure 2. As the runs in quantitative mode for each set of experiments have five different starting years (1969, 1979, 1989, 1999, and 2009), we restrict the travel time to 70 years so that integration periods are exactly the same, making the different runs within a given set of experiments comparable. Furthermore, analyzing a set of experiments has the advantage of covering interannual variations and generating robust results, using integration periods as long as possible (with regard to computation times). The purpose is to analyze runs with the fewest possible

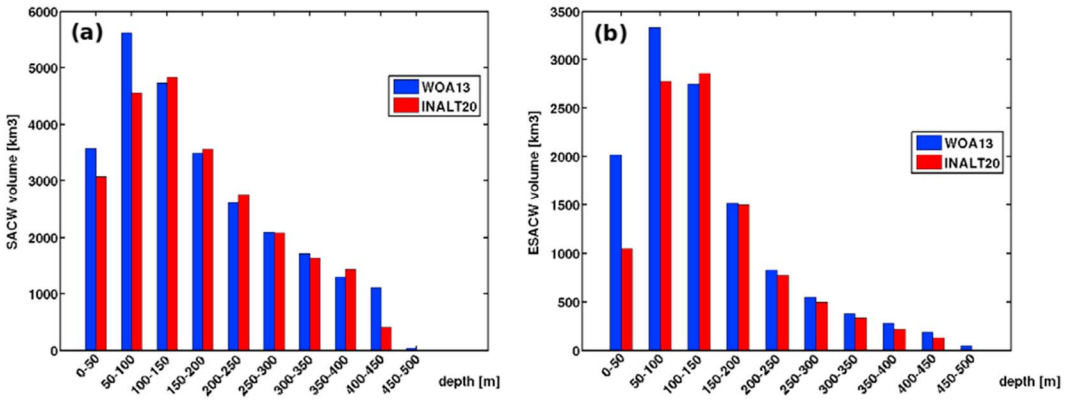

Figure 4. Histogram of the depth-related water volume (km^3) that fulfill the criterion of South Atlantic Central Water in North Benguela (15°S to 27°S) (a) and Eastern South Atlantic Central Water in South Benguela (27°S to 34°S) (b) of INALT20 (red) and WOA13 (blue) between 100 km offshore and the coast, for the decade 1995–2004, interpolated to 1-m vertical intervals and summed up to layers of 50 m thickness.

parcels that do not reach any sampling section and thus could not be evaluated. Furthermore, the variance of the simulated horizontal velocities in the seeding area of the Agulhas Current and in the Benguela upwelling region at 100 m depth during the seeding years covers 99% of their total variance during the whole simulation period. Thus, these five years (1969, 1979, 1989, 1999, and 2009) represent more than 99% of the variance of the transport in this region. As most of the transport variance in the study regions is captured, our results are not sensitive to the chosen seeding years. With this choice of seeding years we do not accidentally cover only years of very weak upwelling or certain Agulhas Current strength but a wide spectra of velocities.

The contributions of water masses are calculated in quantitative mode by taking the total volume of the seeded parcels minus the meanders, the volume of seeded parcels that end at the seeded section/area (in Sverdrup). Depending on travel times and on the length of the ARIANE analysis, there are some parcels that do not end at any section. "Lost" parcels that cannot be accounted for because they do not reach any predefined sampling section are less than 5% in all experiments, except for the Mixed-Layer run for North Benguela where a larger fraction (19.7%) of the transport that leave the seeding section is lost.

3. Results

3.1. Model Validation

The eddy-resolving simulation INALT20 will be shown elsewhere to adequately represent the Agulhas Current system (F. U. Schwarzkopf, personal communication, April 18, 2018). For the purpose of this analysis, we validate the model performance with regard to the central water masses and the upwelling in the BUS.

In the Benguela upwelling region (15°S to 34°S, between the coastline and 100 km offshore), the simulated temperature and salinity profiles are very similar to the observational data set WOA13 (Figure 3) for the period 1995–2004. Both data sets show a warmer and saltier water mass in the North Benguela region than in the South Benguela region. They show comparable vertical profiles, even though the horizontal resolution of both data sets are very different (1/4° for WOA13 and 1/20° for INALT20). The mean temperature difference between INALT20 and WOA13 is 0.6 °C at 10 m depth and 1.4 °C at 100 m depth averaged over the upwelling region. In 10 m depth the temperatures have a cold bias directly at the coast and a warm bias in the rest of the upwelling region, again defined as the area that extents 100 km off the coast (not shown). An overestimation of equatorward winds may cause the negative bias directly at the coast (Veitch et al., 2010; Xu et al., 2014). The general positive bias in 10 and 100 m depth is well known from coupled models, especially in the EBUSs (Richter, 2015). In this ocean-only simulation, the bias might have its origin in a too strong Benguela undercurrent caused by a too deep thermocline in the Angola Current region (Xu et al., 2014). This intense Benguela undercurrent might cause an overestimation of the contribution of water from the equatorial region to North Benguela central water masses and thus enhanced travel times and an underestimation of the contribution from South Benguela via the Lüderitz cell.

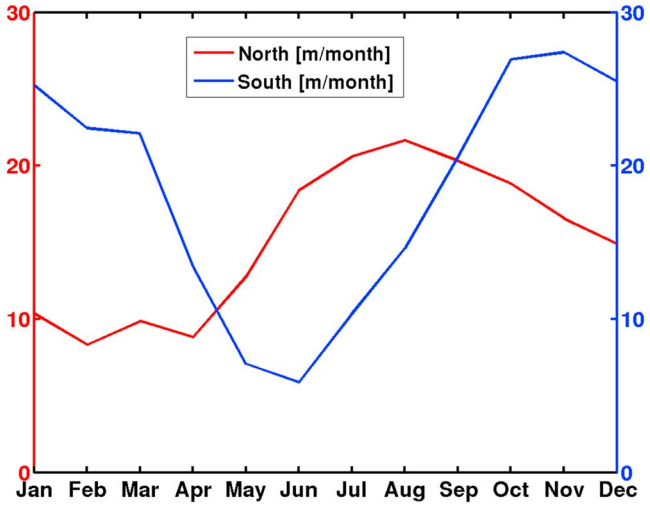

Figure 5. Mean annual cycle of simulated upwelling (vertical velocity) in meters per month for North Benguela (red line, 15°S to 27°S) and South Benguela (blue line, 27°S to 34° S) between the coast and 100 km offshore, in 100 m depth over the simulation period 1958–2009.

We now assess quantitatively the simulated water masses in the region. Figure 4 depicts the water volume in km^3 in which the temperature and salinity criteria of the definition of central water masses SACW in North Benguela and ESACW in South Benguela are fulfilled (SACW: 8.00–16.00 °C, 34.72–35.64 psu; ESACW: 5.95–14.41 °C, 34.41–35.30 psu). Water volumes are calculated by interpolating vertically to 1-m intervals and summing up to layers of 50-m thickness. The histograms of SACW and ESACW agree well, and usual statistical tests (*t* test and *f* test) cannot differentiate their mean and variance. However, in the observational data set WOA13 the central water masses cover a larger volume in the upper 100 m than in the simulation, likely due to discrepancies in horizontal resolution and the difficulties of the model to adequately simulate coastal upwelling. Even with these discrepancies in temperature and salinity and the uncertainty of their causes, the model captures well both the depth range occupied by the central water masses and the depth-dependent variations shown in the profiles of temperature and salinity.

The upwelling itself, defined here as the simulated vertical velocity at 100 m depth, shows an annual cycle and strength, comparable to other model studies (Small et al., 2015; Tim et al., 2015, 2016). Direct comparison to observations is not possible as there are no long-term direct observations of upwelling intensity. However, we compared the modeled SST and temperature in 10 m depth to the HadISST and WOA, respectively. At both depths, the simulation has a cold bias directly at the coast and a warm bias in the rest of the upwelling region. Nevertheless, the upwelling region can be clearly identified in the INALT20 SST and 10-m temperature. Upwelling is strongest in austral winter in North Benguela and in austral summer in South Benguela (Figure 5), as previously found by Shannon and O'Toole (2003). The choice of 100 m depth as representative for the upwelling is supported by the simulated depth of the mixed layer. The mixed-layer depth is here defined as the depth where the density differs by at least 0.01 kg/m^3 from the density at 10 m depth. The simulated mixed-layer depth in the upwelling region is on average 24 m. In only 0.05% of the cases is the mixed-layer depth in the upwelling region below 100 m over the whole simulation period. Furthermore, vertical velocities are strongest in the upper 250 m. Thus, validating the vertical velocity at 100 m depth provides a plausible representation of the upwelling.

3.2. Amount of Agulhas Water in the Benguela Upwelling Region

The variations of the Agulhas leakage and the amount of Agulhas water in the Benguela upwelling region impact the nutrient and oxygen concentrations in the upwelling area.The simulated Agulhas leakage (defined

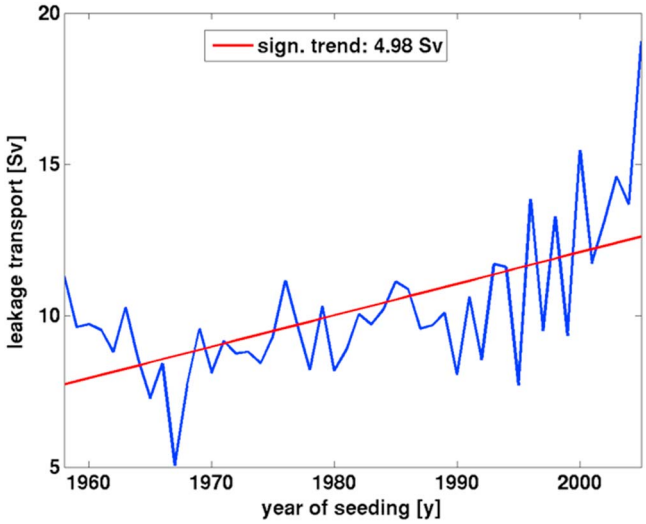

Figure 6. Trend of the Agulhas leakage transport at the Good Hope Line (3–8°E, 45–33°S, and 8–18°E, 33°S). Only parcels reaching the leakage within 5 years are considered.

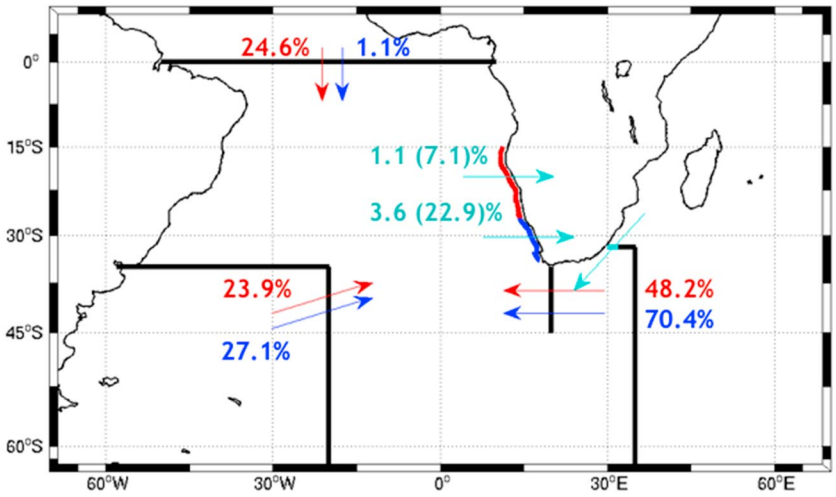

Figure 7. Schematic map of initial (seeding) and final (sampling) sections with the corresponding percentage of volume transport (Sverdrup) that reaches each sampling section. In turquoise is the Agulhas-Benguela experiment. Percentages in brackets refer to the percentage of leakage water. In red is the North Benguela experiment and in blue the South Benguela experiment. Black lines represent the sampling sections as further described in section 2. Arrows indicate the direction of transport at seeding and sampling sections.

as in Biastoch et al., 2008; Durgadoo et al., 2013) is 12.9 Sv, around 20.4% of the Agulhas Current averaged over the period 1995–2005. This matches results of previous studies that analyzed the impact of Agulhas water onto the North Atlantic and the sources of the leakage water (Durgadoo et al., 2017; Rühs et al., 2013). The leakage has significantly increased over this period by 4.98 Sv (Figure 6), as previously found by Biastoch et al. (2009).

The path of the Agulhas water in the South Atlantic, analyzed in the Agulhas-Benguela experiment, gives a first hint at the impact of these variable Indian Ocean water masses on the upwelling region. Around 3.6% of the Agulhas Current water (seeded in the Agulhas Current at 32°S) and around 22.9% of the leakage water (water that passes the Good Hope Line and leaves the Agulhas Current System) reach the South Benguela upwelling region (Figure 7). In contrast, only 1.1% (7.1%) of the Agulhas water (leakage water) arrives in the North Benguela upwelling region.

3.3. Origin and Pathways of Central Water Masses

In addition to the amount of Agulhas water reaching the upwelling regions, we are interested in its contribution to the central water masses in the BUS and the path that the central water masses take before entering the upwelling region.

Analyzing the contribution of Agulhas water to the Benguela central water masses SACW and ESACW reveals the importance of the Agulhas leakage as a source for the upwelling water masses, and shows that a large proportion of water mass in the upwelling region did originate in the Agulhas Current. Seeding in the two upwelling regions and tracking the central water masses backward in time shows the strong contribution of the Agulhas Current not only on the South Benguela upwelling region, but on both upwelling areas. Our Lagrangian analyses of the origins of central waters in South Benguela (North Benguela) show that on average from 1.68 Sv (2.25 Sv) only 0.45 Sv, that is, 27.1% (0.54 Sv, 23.9%) originate directly from the region around the Brazil-Malvinas Confluence Zone, while 1.18 Sv, that is, 70.4% (1.09 Sv, 48.2%) of the central waters stem directly from the Agulhas region (Figure 7). Water from north of the equator contributes 24.6% to the SACW in North Benguela, but only negligibly to South Benguela ESACW. The residual 1–4% of the water volume do not reach any sampling section (Figure 7).

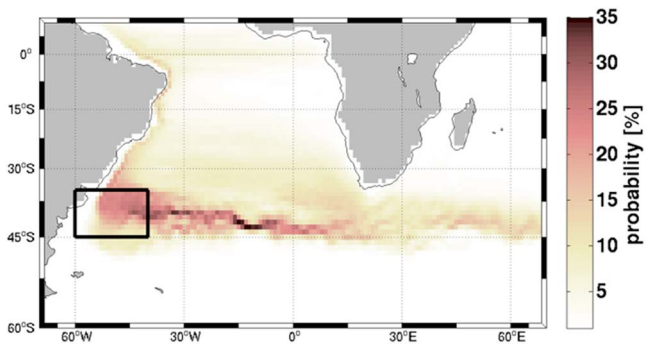

Figure 8. Percentage of parcels seeded in the Brazil-Malvinas Confluence Zone (formation region) and calculated forward passing a 1° grid box at least once during the whole simulation period (1958–2009).

Trajectory analyses of the qualitative mode depict the pathways of SACW and ESACW backward in time on the one hand, and of water from the

Table 1
Transport (Sv), Percentage (%) of Contributions, and Travel Times (y) of the Experiments North Benguela and South Benguela for the Five Different Starting Years

	1969	1979	1989	1999	2009
North Benguela					
Total-meander transport (Sv)	2.43	2.17	2.32	2.46	1.86
Leakage contribution (Sv)	1.20	1.06	1.19	1.14	0.84
Leakage contribution (%)	49.4	48.8	51.3	46.3	45.2
Formation contribution (Sv)	0.60	0.51	0.56	0.64	0.39
Formation contribution (%)	24.7	23.5	24.1	26.0	21.0
Time from leakage to North B. (y)	5.0	6.5	4.4	5.9	8.1
South Benguela					
Total-meander transport (Sv)	1.75	1.74	1.57	1.94	1.39
Leakage contribution (Sv)	1.16	1.23	1.11	1.43	0.98
Leakage contribution (%)	66.3	70.7	70.7	73.7	70.5
Formation contribution (Sv)	0.54	0.45	0.42	0.49	0.37
Formation contribution (%)	30.9	25.9	26.8	25.3	26.6
Time from leakage to South B. (y)	1.9	1.6	1.3	0.9	1.4

formation region and of the Agulhas Current water forward in time on the other hand. Contrary to our hypothesis, most of the central water mass from the confluence zone does not directly reach the upwelling region, but flows into the Indian Ocean, and thus may reach Benguela as Agulhas leakage water only later. This is shown in Figure 8 displaying the forward pathway of the parcels seeded in the Brazil-Malvinas Confluence Zone. Calculating the percentage of parcels reaching the upwelling areas suggests that only 10.8% of the parcels from the confluence arrives in South Benguela and only 7.9% reach North Benguela. But it has to be kept in mind that this analysis covers only the 52 years simulation period and that water from the formation region may require even longer travel times to reach the upwelling region. This, however, would again hint at an extra loop through the Indian Ocean and this is unlikely to have a strong influence on the transport to the upwelling region with the Benguela Current.

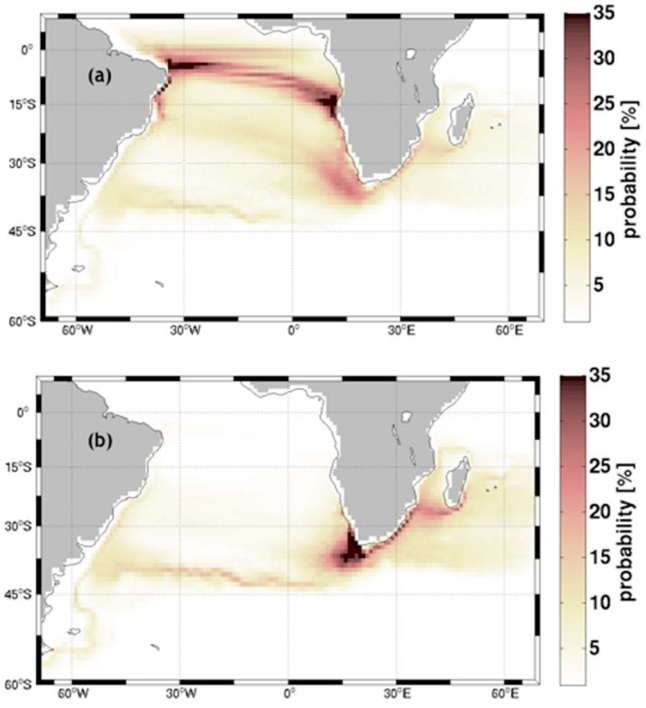

Figure 9. Percentage of parcels seeded in North Benguela (a) and South Benguela (b) and calculated backward passing a 1° grid box at least once during the whole simulation period (1958–2009).

When comparing the five cases with different seeding years of the North and South Benguela experiments, it is noteworthy that for North and South Benguela the total volume transport of central waters into the upwelling region (the transport at the seeding section in the corresponding seeding year) and the individual volumetric contributions of waters with Agulhas origin vary roughly proportionally (Table 1). Total volume transport refers to the total seeded transport minus the meanders, the transport that ends at the seeding section. Larger transport of central waters into North and South Benguela goes along with larger volumetric contributions of waters with Agulhas origin. However, the here discussed Lagrangian analyses are not sufficient to unequivocally determine a link between Agulhas leakage strength and the Agulhas contribution to South Benguela central waters. In principal, a larger Agulhas contribution could stem from a preceded increase in Agulhas leakage transport and/or from a higher percentage of Agulhas leakage waters reaching Benguela due to changes in the subtropical gyre circulation (even if Agulhas leakage itself stays constant or decreases).

For North Benguela, the volumetric contribution of waters with Agulhas origin to the total transport of central waters into the upwelling region seems to be locked to the average transit time between South of Africa and North Benguela: The shorter the transit time, the larger the Agulhas contribution. In the two years 1969 and 1989 with the largest Agulhas

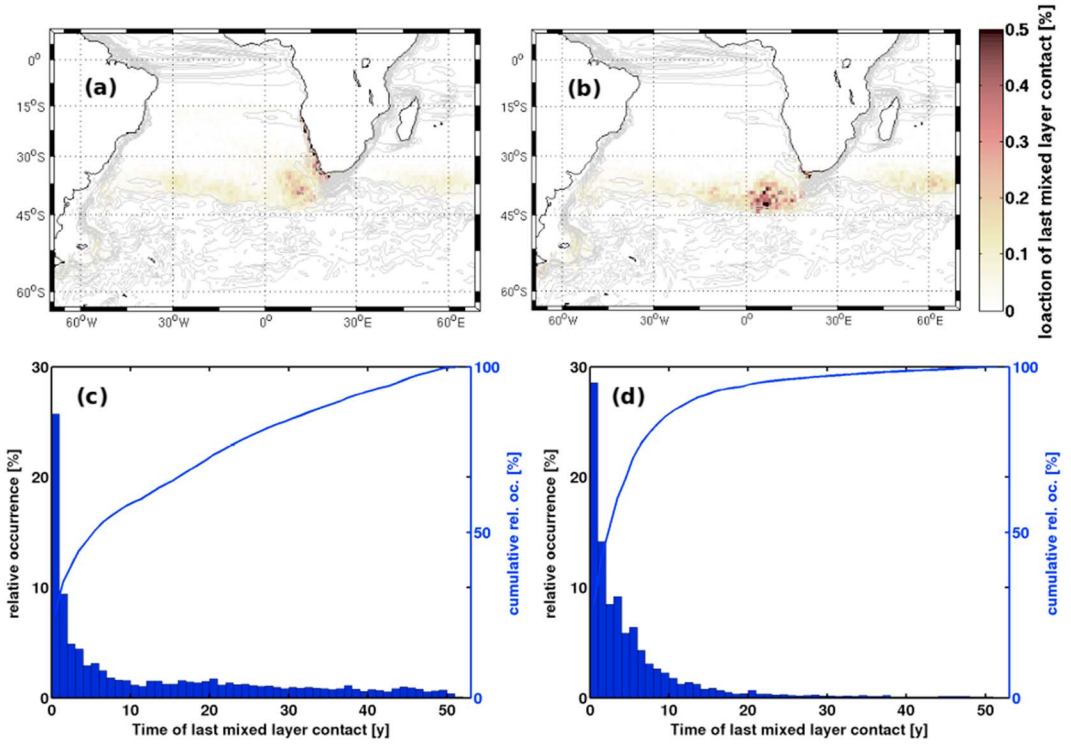

Figure 10. Location of last mixed-layer contact (in %) of the water masses that reach North Benguela (a) and South Benguela (b) in a 1° grid box with gray lines representing the mean circulation (averaged over the simulation period 1958–2009), and their travel time from last mixed-layer contact when reaching North Benguela (c) and South Benguela (d).

contributions of 1.2 Sv each (constituting 49.4% and 51.3% of the total transport of central waters into the upwelling region in 1969 and 1989, respectively) virtual fluid parcels took on average 5.0 and 4.4 years for the transit, respectively (Table 1). In the year 2009 with the smallest Agulhas contribution of 0.84 Sv (45.2% of total central water transport) on average 8.1 years were needed for the transit. We hypothesize that this link may indicate variability in biogeochemical properties of SACW imposed by variable Agulhas contribution. For South Benguela travel times are very similar in all five cases ranging only between 1 and 2 years.

The North and South Benguela central water masses are thus dominantly fed by the Agulhas Current (Figure 9). Differences arise along the two pathways: North Benguela upwelling feed water originating from the Agulhas current crosses the entire South Atlantic and enters the upwelling region from the north. It does not take the direct path through the Lüderitz upwelling cell that separates both upwelling regions at 27°S, as confirmed by the Lüderitz run, where we seeded the parcels at the southern border of South Benguela (34°S) between the coast and 8°E. Only 19.1% of these parcels cross the 27°S latitude boundary between South Benguela and North Benguela, whereas 80.9% leave the South Benguela upwelling region and flow westward with the Benguela Current or with the Ekman transport.

3.4. Age of the Water Masses in the BUS

The water of the North BUS travels a longer way from the formation region and the Agulhas leakage than the South Benguela central water mass. Accordingly, the computed travel times are on average longer for North than for South Benguela. In this section we estimate the age of the water parcels, defined as the time from the last time the parcel has been in the simulated mixed layer. The mixed-layer depth is here defined as the level where the density differs by at least 0.01 kg/m^3 from the density at 10 m depth.

The ages of the central water masses in North and South Benguela show clear differences. The upwelling water mass in North Benguela is on average 13.1 years old, whereas the central water mass in South Benguela has an age of around 5.6 years (Figure 10).

We analyzed the horizontal location of the last position of the water parcels in the mixed layer. Figure 10 shows that both water masses originate from mainly two regions, a region in the Cape Basin and along the

South African coast. Ventilation in the Cape Basin, north of the Subtropical Front and west of the Agulhas Retroflection, might occur here due to mixing of water transported eastward with the South Atlantic Current and Agulhas rings transporting Indian Ocean water into the Atlantic. The mixed-layer contact in the upwelling region itself might be due to recirculation. As the variability of the vertical velocity in the upwelling region is high and only 2.5% of the parcels for North Benguela and 0.2% for South Benguela are seeded within the mixed layer, fluctuations in the vertical transport probably cause the ventilation of the central water masses in the Benguela upwelling region. The formation region in the Brazil-Malvinas Confluence Zone is not a frequent area for last mixed-layer contact. This implies that central water formed in this region reenters the ventilated mixed layer before reaching the Benguela upwelling region or needs longer travel times. For both, North and South Benguela, 45.3–50.0% of the seeded transport has been in the mixed layer within the simulation's nest domain. A large fraction (26.6% for North and 44.6% for South Benguela) originate from the Indian Ocean east of 70°E and small amounts (2.7% and 5.0%) originate from the Pacific Ocean through Drake Passage. It has to be kept in mind that for the North Benguela experiment 19.7% of the seeded transport do not reach any sampling section.

4. Discussion and Conclusion

In the ocean simulation INALT20 driven by atmospheric reanalysis (COREv2) over the period 1958–2009, the Agulhas Current and Agulhas leakage are the origins of the central water masses that are upwelled in the BUS. The contribution of Indian Ocean water is 70.4% of the feed water mass in the South Benguela region, and even in the North Benguela region 48.2% of the water mass has its origin east of 20°E.

The remaining water mass fractions originate from the Brazil-Malvinas Confluence Zone (around 25% in both North and South Benguela) and from the equatorial current system that has a negligible contribution for South Benguela, but 24.6% for the central water mass in North Benguela.

Our analysis of this ocean simulation supports the conclusions derived from observations of Mohrholz et al. (2008) that the central water masses in the North and South Benguela upwelling regions differ in their temperature and salinity. Furthermore, the different pathways into the upwelling region is as was hypothesized by Mohrholz et al. (2008): Water from the confluence zone mixes with Agulhas water to form South Benguela ESACW and flows with the Benguela Current into the upwelling region. In contrast, North Benguela SACW enters the upwelling region largely by the equatorial current system and only a smaller fraction crosses the Lüderitz cell, the boundary between the two subsystems.

The origin of the water masses in the BUS is much more frequently the Agulhas Current than the subduction region in the Brazil-Malvinas Confluence Zone. A large fraction of the subducted water in this region flows eastward with the South Atlantic Current and returns with the Agulhas Return Current to the Indian Ocean. Therefore, our study suggests that the Brazil-Malvinas subduction region is of minor importance in controlling the composition of water masses in the BUS.

These differences are expressed in estimated water age and associated biogeochemical properties. The North Benguela central water mass takes a longer path from the leakage and from the formation region in the confluence zone than South Benguela central water mass. SACW thus is older than ESACW, and the location of the last mixed-layer contact of both water masses is often southwest of the Cape of Good Hope, in the Cape Basin, prior to mixed-layer contacts in the upwelling region itself. Thus, the ventilation of the central water masses happens close to the African continent, where gas exchange equilibria with the atmosphere are attained and nutrients are depleted. ESACW upwelling in South Benguela is, therefore, quite young with an average age of 5.6 years, and oxygen utilization, CO_2 and nutrient build-up from remineralization of sinking organic matter are significantly lower than in SACW. Travel times from last ventilation of that water on the way to North Benguela are twice as long—on average 13.1 years. This age difference can help explaining the contrasting nutrient, CO_2 and oxygen properties of the upwelling feed water masses in the North and South Benguela (Emeis et al., 2018).

The Agulhas leakage accounts for an average of 20% of the Agulhas Current System and our study shows the strong link between the Agulhas Current water and the central water masses that feed upwelling in the Benguela system. The leakage has significantly increased in this simulation over the last five decades, with a quite stable leakage until 1990 and a pronounced increase during the last 20 years (see Figure 6), agreeing with the results of Biastoch et al. (2009) based on a previous version of the model configuration analyzed

here. The intensification of the leakage in the past, as a consequence of intensified extratropical westerly winds (Durgadoo et al., 2013), is predicted to continue in the future (Biastoch & Böning, 2013). We hypothesize that this proposed strengthening of the leakage due to wind changes in the future might lead to further increase the Agulhas water contribution in the upwelling region off southwest Africa, as the volume transport into the upwelling regions is larger if the contribution of the Agulhas is larger. Furthermore, travel times of central water with Agulhas origin into North Benguela are shorter when the Agulhas contribution is larger. Thus, variations and increases in the Agulhas leakage due to changes in the westerlies over the Indian Ocean might increase the proportion of Agulhas water in both upwelling regions and decrease (at increasing oxygen inventories) the nutrient and CO_2 concentrations of the central water masses of the BUS; if the westerlies wind system indeed evolves in the future as predicted, it is to be expected that the effects will be stronger in the northern Benguela than in the southern Benguela.

However, the poleward shift and intensification of the westerlies over the Southern Hemisphere is currently intensely studied (Fyfe & Saenko, 2006; Hande et al., 2012; Russell et al., 2006; Swart & Fyfe, 2012; Yang et al., 2007). The future evolution of these trends is still under debate. The ongoing increase in greenhouse gas concentration would be responsible for a further southward displacement of the westerlies (Watson et al., 2012). On the other hand, the ozone recovery over Antarctica after the implementation of emission reduction of fluorocarbon compounds and subsequently reduced concentrations in the polar stratosphere are thought to counteract this effect (Watson et al., 2012). Clearly, more research is needed to establish which factor will be dominant in the future: Since this remote control has considerable impact on the Agulhas leakage, the composition and travel times of the water masses feeding the Benguela upwelling, it also controls nutrient and oxygen content of the upwelling water, the entire rich ecosystem and marine resources of the BUS.

Our analysis supports the age and pathways of the central water masses in the BUS previously estimated based on observations and shows the large contribution of Agulhas water for the past five decades. The positive trend in leakage fits changes in westerlies in the recent past, and, thus, our study hints at how the contribution of Agulhas water to the BUS might change in the future.

Acknowledgments
The model simulation has been performed at the North-German Supercomputing Alliance (HLRN). We thank the developers of Ariane. The Ariane-v2.2.8 Lagrangian software tool was downloaded from http://www.univ-brest.fr/lpo/ariane/. World Ocean Atlas 2013 data for model validation was downloaded from https://www.nodc.noaa.gov/OC5/woa13/. The ARIANE-derived output are available on request. The project received funding by the German Federal Ministry of Education and Research (BMBF) of the SPACES-AGULHAS project, grants 03F0750A and 03F0750C, by the Cluster of Excellence 80 The Future Ocean within the framework of the Excellence Initiative by the Deutsche Forschungsgemeinschaft (DFG) on behalf of the German federal and state governments, grant CP1412, by the Helmholtz-Zentrum Geesthacht, and by the University of Hamburg.

References

Bakun, A., Field, D. B., Redondo-Rodriguez, A., & Weeks, S. J. (2010). Greenhouse gas, upwelling-favorable winds, and the future of coastal ocean upwelling ecosystems. *Global Change Biology*, *16*(4), 1213–1228. https://doi.org/10.1111/j.1365-2486.2009.02094.x

Barnier, B., Madec, G., Penduff, T., Molines, J.-M., Treguier, A.-M., Le Sommer, J., et al. (2006). Impact of partial steps and momentum advection schemes in a global ocean circulation model at eddy-permitting resolution. *Ocean Dynamics*, *56*(5), 543–567. https://doi.org/10.1007/s10236-006-0082-1

Beal, L. M., & Bryden, H. L. (1997). Observations of an Agulhas Undercurrent. *Deep Sea Research Part I: Oceanographic Research Papers*, *44*(9), 1715–1724. https://doi.org/10.1016/S0967-0637(97)00033-2

Beal, L. M., De Ruijter, W. P. M., Biastoch, A., Zahn, R., & SCOR/WCRP/IAPSO Working Group 136 (2011). On the role of the Agulhas system in ocean circulation and climate. *Nature*, *472*(7344), 429–436. https://doi.org/10.1038/nature09983

Biastoch, A., & Böning, C. W. (2013). Anthropogenic impact on Agulhas leakage. *Geophysical Research Letters*, *40*, 1138–1143. https://doi.org/10.1002/grl.50243

Biastoch, A., Böning, C. W., Schwarzkopf, F. U., & Lutjeharms, J. (2009). Increase in Agulhas leakage due to poleward shift of Southern Hemisphere westerlies. *Nature*, *462*(7272), 495–498. https://doi.org/10.1038/nature08519

Biastoch, A., Durgadoo, J. V., Morrison, A. K., Van Sebille, E., Weijer, W., & Griffies, S. M. (2015). Atlantic multi-decadal oscillation covaries with Agulhas leakage. *Nature Communications*, *6*(10082). https://doi.org/10.1038/ncomms10082

Biastoch, A., Lutjeharms, J. R. E., Böning, C. W., & Scheinert, M. (2008). Mesoscale perturbations control inter-ocean exchange south of Africa. *Geophysical Research Letters*, *35*, L20602. https://doi.org/10.1029/2008GL035132

Blanke, B., & Raynaud, S. (1997). Kinematics of the Pacific equatorial undercurrent: An Eulerian and Lagrangian approach from GCM results. *Journal of Physical Oceanography*, *27*(6), 1038–1053. https://doi.org/10.1175/1520-0485(1997)027<1038:KOTPEU>2.0.CO;2

Boyer, T. P., Antonov, J. I., Baranova, O. K., Coleman, C., Garcia, H. E., Grodsky, A., et al. (2013). World ocean database 2013. In S. Levitus & A. Mishonov (Eds.), *NOAA Atlas NESDIS 72* (pp. 209). Silver Spring, MD. https://doi.org/10.7289/V5NZ85MT

Castellanos, P., Campos, E. J. D., Piera, J., Sato, O. T., & Silva Dias, M. A. F. (2017). Impacts of Agulhas leakage on the tropical atlantic western boundary systems. *Journal of Climate*, *30*(17), 6645–6659. https://doi.org/10.1175/JCLI-D-15-0878.1

Debreu, L., Vouland, C., & Blayo, E. (2008). AGRIF: Adaptive grid refinement in Fortran. *Computers & Geosciences*, *34*(1), 8–13. https://doi.org/10.1016/j.cageo.2007.01.009

Durgadoo, J. V., Loveday, B. R., Reason, C. J. C., Penven, P., & Biastoch, A. (2013). Agulhas leakage predominantly responds to the Southern Hemisphere westerlies. *Journal of Physical Oceanography*, *43*(10), 2113–2131. https://doi.org/10.1175/JPO-D-13-047.1

Durgadoo, J. V., Rühs, S., Biastoch, A., & Böning, C. W. B. (2017). Indian Ocean sources of Agulhas leakage. *Journal of Geophysical Research: Oceans*, *122*, 3481–3499. https://doi.org/10.1002/2016JC012676

Emeis, K., Eggert, A., Flohr, A., Lahajnar, N., Nausch, G., Neumann, A., et al. (2018). Biogeochemical processes and turnover rates in the Northern Benguela upwelling system. *Journal of Marine Systems*, *188*, 63–80. https://doi.org/10.1016/j.jmarsys.2017.10.001

Fyfe, J. C., & Saenko, O. A. (2006). Simulated changes in the extratropical Southern Hemisphere winds and currents. *Geophysical Research Letters*, *33*, L06701. https://doi.org/10.1029/2005GL025332

Gordon, A. L. (1986). Interocean exchange of thermocline water. *Journal of Geophysical Research*, *91*(C4), 5037–5046. https://doi.org/10.1029/JC091iC04p05037

Gordon, A. L., Weiss, R. F., Smethie, W. M., & Warner, M. J. (1992). Thermocline and intermediate water communication between the south Atlantic and Indian oceans. *Journal of Geophysical Research*, *97*(C5), 7223–7240. https://doi.org/10.1029/92JC00485

Hande, L. B., Siems, S. T., & Manton, M. J. (2012). Observed trends in wind speed over the Southern Ocean. *Geophysical Research Letters*, *39*, L11802. https://doi.org/10.1029/2012GL051734

Large, W. G., & Yeager, S. G. (2009). The global climatology of an interannually varying air–sea flux data set. *Climate Dynamics*, *33*(2), 341–364. https://doi.org/10.1007/s00382-008-0441-3

Lübbecke, J. F., Durgadoo, J. V., & Biastoch, A. (2015). Contribution of increased Agulhas leakage to tropical Atlantic warming. *Journal of Climate*, *28*(24), 9697–9706. https://doi.org/10.1175/JCLI-D-15-0258.1

Madec, G. (2008). *NEMO Ocean Engine*. France: Note du Pôle de modélisation, Institut Pierre-Simon Laplace (IPSL). No 27, ISSN No 1288-1619.

Mohrholz, V., Bartholomae, C. H., Van der Plas, A. K., & Lass, H. U. (2008). The seasonal variability of the northern Benguela undercurrent and its relation to the oxygen budget on the shelf. *Continental Shelf Research*, *28*(3), 424–441. https://doi.org/10.1016/j.csr.2007.10.001

Pauly, D., & Christensen, V. (1995). Primary production required to sustain global fisheries. *Nature*, *374*(6519), 255–257. https://doi.org/10.1038/376279b0

Poole, R., & Tomczak, M. (1999). Optimum multiparameter analysis of the water mass structure in the Atlantic Ocean thermocline. *Deep Sea Research Part I: Oceanographic Research Papers*, *46*(11), 1895–1921. https://doi.org/10.1016/S0967-0637(99)00025-4

Richter, I. (2015). Climate model biases in the eastern tropical ocean: Causes, impacts and ways forward. *WIREs Climate Change*, *6*, 345–358. https://doi.org/10.1002/wcc.338

Rühs, S., Durgadoo, J. V., Behrens, E., & Biastoch, A. (2013). Advective timescales and pathways of Agulhas leakage. *Geophysical Research Letters*, *40*, 3997–4000. https://doi.org/10.1002/grl.50782

Russell, J. L., Dixon, K. W., Gnanadesikan, A., Stouffer, R. J., & Toggweiler, J. R. (2006). The Southern Hemisphere westerlies in a warming world: Propping open the door to the deep ocean. *Journal of Climate*, *19*(24), 6382–6390. https://doi.org/10.1175/JCLI3984.1

Shannon, L. V. (1985). The Benguela ecosystem part I: Evolution of the Benguela, physical features and processes. *Oceanography and Marine Biology: An Annual Review*, *23*, 105–182.

Shannon, L. V., & O'Toole, M. J. (2003). Sustainability of the Benguela: ex Africa semper aliquid novi. In *Large marine ecosystems of the world: Trends in exploitation, protection and research* (pp. 227–253). Amsterdam: Elsevier.

Small, R. J., Curchitser, E., Hedstrom, K., Kauffman, B., & Large, W. G. (2015). The Benguela upwelling system: Quantifying the sensitivity to resolution and coastal wind representation in a global climate model. *Journal of Climate*, *28*(23), 9409–9432. https://doi.org/10.1175/JCLI-D-15-0192.1

Stramma, L., & England, M. (1999). On the water masses and mean circulation of the South Atlantic Ocean. *Journal of Geophysical Research*, *104*(C9), 20,863–20,883. https://doi.org/10.1029/1999JC900139

Swart, N. C., & Fyfe, J. C. (2012). Observed and simulated changes in the Southern Hemisphere surface westerly wind-stress. *Geophysical Research Letters*, *39*, L16711. https://doi.org/10.1029/2012GL052810

Tim, N., Zorita, E., & Hünicke, B. (2015). Decadal variability and trends of the Benguela upwelling system as simulated in a high-resolution ocean simulation. *Ocean Science*, *11*(3), 483–502. https://doi.org/10.5194/os-11-483-2015

Tim, N., Zorita, E., Hünicke, B., Yi, X., & Emeis, K.-C. (2016). The importance of external climate forcing for the variability and trends of coastal upwelling in past and future climate. *Ocean Science*, *12*(3), 807–823. https://doi.org/10.5194/os-12-807-2016

van Sebille, E., Griffies, S. M., Abernathey, R., Adams, T. P., Berloff, P., Biastoch, A., et al. (2018). Lagrangian ocean analysis: Fundamentals and practices. *Ocean Modelling*, *121*, 49–75. https://doi.org/10.1016/j.ocemod.2017.11.008

Veitch, J. A., & Penven, P. (2017). The role of the Agulhas in the Benguela Current system: A numerical modeling approach. *Journal of Geophysical Research: Oceans*, *122*, 3375–3393. https://doi.org/10.1002/2016JC012247

Veitch, J., Penven, P., & Shillington, F. (2010). Modeling equilibrium dynamics of Benguela current system. *Journal of Physical Oceanography*, *40*, 1942–1964. https://doi.org/10.1175/2010JPO4382.1

Watson, P. A. G., Karoly, D. J., Allen, M. R., Faull, N., & Lee, D. S. (2012). Quantifying uncertainty in future Southern Hemisphere circulation trends. *Geophysical Research Letters*, *39*, L23708. https://doi.org/10.1029/2012GL054158

Xu, Z., Li, M., Patricola, C. M., & Chang, P. (2014). Oceanic origin of southeast tropical Atlantic biases. *Climate Dynamics*, *43*(11), 2915–2930. https://doi.org/10.1007/s00382-013-1901-y

Yang, X.-Y., Huang, R. X., & Wang, D. X. (2007). Decadal changes of wind stress over the Southern Ocean associated with Antarctic ozone depletion. *Journal of Climate*, *20*(14), 3395–3410. https://doi.org/10.1175/JCLI4195.1